PERGAMON

International Journal of Heat and Mass Transfer 44 (2001) 4267–4275

International Journal of HEAT and MASS TRANSFER

www.elsevier.com/locate/ijhmt

# Mixed convection with viscous dissipation in an inclined channel with prescribed wall temperatures

A. Barletta *, E. Zanchini

*Dipartimento di Ingegneria Energetica, Nucleare e del Controllo Ambientale (DIENCA), Università di Bologna, Viale Risorgimento 2, I-40136 Bologna, Italy*

Received 19 October 2000; received in revised form 31 January 2001

**Abstract**

The fully developed laminar mixed convection with viscous dissipation in an inclined channel with prescribed wall temperatures is studied analytically. The mean fluid temperature is assumed as the reference temperature. Two perturbation expansions are considered. In the first, the forced convection with viscous dissipation is assumed as a starting condition and the effects of buoyancy for fixed values of the Brinkman number are studied. In the second, starting from the solution for mixed convection without viscous dissipation, the effects of the Brinkman number for fixed values of the Grashof number are analysed. The different solution methods allow a cross-check of the results. The dimensionless velocity field, the dimensionless temperature field, the dimensionless pressure field, the friction factors and the Nusselt numbers are determined and discussed. The results show that viscous dissipation enhances the effects of buoyancy and vice versa. 

## 1. Introduction

Recently, a wide literature on laminar mixed convection in either vertical or horizontal channels and tubes has been developed. The main technical applications of these researches concern cooling systems for electronic devices and solar energy thermal conversion. Many results available in the literature are collected in [1]. In particular, the fully developed mixed convection in vertical channels has been studied analytically by Aung and Worku [2], Cheng et al. [3], Hamadah and Wirtz [4], Barletta and Zanchini [5]. In [5], the solutions obtained in [2–4] have been extended to broader boundary conditions; moreover, a method for the choice of the reference fluid temperature which is employed in the linearisation of the equation of state $\rho = \rho(T)$ has been determined. The linear stability of fully developed laminar mixed convection in vertical channels has been studied by Chen and Chung, for the boundary conditions of linearly varying wall temperatures [6] and uniform but different wall temperatures [7]. In all the studies quoted above, the viscous dissipation within the fluid has been neglected. The effect of viscous dissipation on fully developed mixed convection in vertical channels or vertical circular tubes, for several boundary conditions, has been studied by Barletta [8–11] and by Zanchini [12].

A few studies concern mixed convection in inclined channels. An analytical solution for laminar mixed convection in a channel with a uniform wall heat flux, heated fluid and downward flow is presented by Lavine [13]. The solution does not depend monotonically on the tilt angle. A study of the same author on the stability of the flow, for the problem quoted above, concludes that the flow is unstable for every value of the Rayleigh number [14]. An experimental work on laminar mixed convection in an inclined tube, with heated fluid, downward flow and uniform wall temperature, shows a stable flow even when flow-reversal occurs [15]. A numerical study of the inlet region for laminar mixed convection in an inclined tube with a uniform wall temperature is presented in [16]. In all the calculations on inclined channels quoted above the viscous dissipation in the fluid has been neglected.

In this paper, the fully developed and laminar mixed convection with viscous dissipation in an inclined

* Corresponding author. Tel.: +39-51-2093295; fax: +39-51-2093296.

*E-mail address:* antonio.barletta@mail.ing.unibo.it (A. Barletta).

0017-9310/01/$ - see front matter 
PII: S0017-9310(01)00071-0

**Nomenclature**

| | |
|---|---|
| $Br$ | Brinkman number defined in Eq. (13) |
| $Br_{\max}$ | radius of convergence of the series defined by Eqs. (38)–(41) |
| $C$ | derivative of $P$ with respect to $X$ (Pa m$^{-1}$) |
| $f_1$ | friction factor at $y=-1$ |
| $f_2$ | friction factor at $y=1$ |
| $F$ | part of $P$ which is a function of $Y$ (Pa) |
| $g$ | modulus of the acceleration due to gravity (m s$^{-2}$) |
| $Gr$ | Grashof number defined in Eq. (13) |
| $Gr_T$ | Grashof number defined in Eq. (30) |
| $k$ | thermal conductivity (W m$^{-1}$ K$^{-1}$) |
| $L$ | half of the channel width (m) |
| $Nu_1$ | Nusselt number at $y=-1$ defined in Eq. (21) |
| $Nu_2$ | Nusselt number at $y=1$ defined in Eq. (21) |
| $p$ | pressure (Pa) |
| $P$ | difference between the pressure and the hydrostatic pressure (Pa) |
| $Re$ | Reynolds number defined in Eq. (13) |
| $T$ | temperature (K) |
| $T_0$ | reference fluid temperature defined by Eq. (4) (K) |
| $T_1$ | temperature at $y=-1$(K) |
| $T_2$ | temperature at $y=1$ (K) |
| $u$ | $=U/U_0$, dimensionless velocity component in the $X$-direction |
| $u_n$ | $n$th coefficient of the perturbation series considered in Section 3 |
| $u_{T_n}$ | $n$th coefficient of the perturbation series defined by Eq. (38) |
| $U$ | velocity component in the $X$-direction (m s$^{-1}$) |
| $U_0$ | mean value of $U$ defined in Eq. (14) (m s$^{-1}$) |
| $X$ | streamwise coordinate (m) |
| $y$ | $=Y/L$, dimensionless transverse coordinate |
| $Y$ | transverse coordinate |

*Greek symbols*

| | |
|---|---|
| $\beta$ | thermal expansion coefficient (K$^{-1}$) |
| $\Delta T$ | reference temperature difference defined in Eq. (14) |
| $\varepsilon$ | dimensionless parameter defined in Eq. (13) |
| $\varepsilon_{\max}$ | radius of convergence of the series considered in Section 3 |
| $\varepsilon_T$ | dimensionless parameter defined in Eq. (30) |
| $\eta$ | dimensionless parameter defined in Eq. (13) |
| $\eta_n$ | $n$th coefficient of the perturbation series considered in Section 3 |
| $\eta_T$ | dimensionless parameter defined in Eq. (30) |
| $\eta_{T_n}$ | $n$th coefficient of the perturbation series defined by Eq. (41) |
| $\theta$ | dimensionless temperature defined in Eq. (13) |
| $\theta_n$ | $n$th coefficient of the perturbation series considered in Section 3 |
| $\theta_T$ | dimensionless temperature defined in Eq. (30) |
| $\theta_{T_n}$ | $n$th coefficient of the perturbation series defined by Eq. (39) |
| $\lambda$ | dimensionless pressure drop coefficient defined in Eq. (13) |
| $\lambda_n$ | $n$th coefficient of the perturbation series considered in Section 3 |
| $\lambda_{T_n}$ | $n$th coefficient of the perturbation series defined by Eq. (40) |
| $\mu$ | dynamic viscosity (Pa s) |
| $\rho$ | mass density (kg m$^{-3}$) |
| $\rho_0$ | mass density at $T=T_0$ (kg m$^{-3}$) |
| $\varphi$ | tilt angle (rad) |
| $\Omega$ | dimensionless function of $y$ defined by Eqs. (22) and (23) |
| $\Omega_T$ | dimensionless function of $y$ defined by Eqs. (36) and (37) |

channel with isothermal walls is studied. According to the prescriptions developed in [5], the mean fluid temperature in each cross-section, which turns out to be invariant along the flow, is chosen as the reference fluid temperature. In each point, for given values of Grashof, Reynolds and Brinkman numbers, any dimensionless quantity turns out to be a monotonic function of the tilt angle.

## 2. Mathematical model

Let us consider a Newtonian fluid, which undergoes a steady and laminar flow in a parallel-plane channel with a tilt angle $\varphi$ with respect to a vertical direction. A sketch of the system under exam and of the coordinate axes is reported in Fig. 1. The channel walls are isothermal, with prescribed temperatures $T_1$ and $T_2$. Let us assume that the velocity field is parallel and such that only the component $U$ along the $X$ direction is non-zero. According to the Boussinesq approximation, the velocity field will be considered as solenoidal. Therefore $\partial U/\partial X=0$, the velocity field depends only on $Y$ and no acceleration is present. The momentum balance equations along $X$ and along $Y$ can be written as

$$-\frac{\partial P}{\partial X}+\rho_0 g\beta(T-T_0)\cos\varphi+\mu\frac{\mathrm{d}^2U}{\mathrm{d}Y^2}=0, \tag{1}$$

$$-\frac{\partial P}{\partial Y}+\rho_0 g\beta(T-T_0)\sin\varphi=0, \tag{2}$$

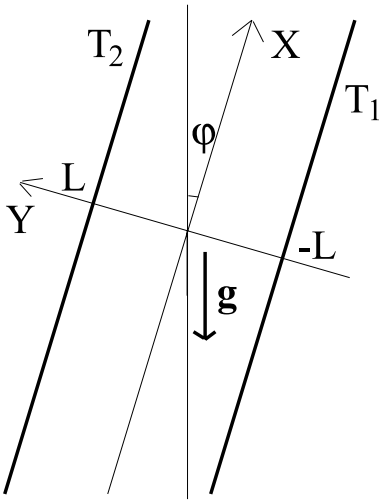


Fig. 1. Sketch of the channel and of the coordinate system.

where $P$ is the difference between the pressure and the hydrostatic pressure

$$P = p + \rho_0 g(X\cos\varphi + Y\sin\varphi) \tag{3}$$

and $T_0$ is the reference temperature, defined as

$$T_0 = \frac{1}{2L}\int_{-L}^{L} T\,\mathrm{d}Y. \tag{4}$$

The condition $\partial U/\partial X = 0$, which is a consequence of the Boussinesq approximation, and the local mass balance equation yield

$$\frac{\partial}{\partial X}[\rho(X,Y)U(Y)] = 0 \tag{5}$$

and thus $\partial\rho/\partial X = 0$. Since the Boussinesq approximation implies also that the mass density depends only on temperature, one concludes that $\partial T/\partial X = 0$. On account of Eq. (4), also the reference fluid temperature $T_0$ is independent of $X$ and thus is a constant. The results obtained above imply that the energy balance equation can be written as

$$k\frac{\mathrm{d}^2T}{\mathrm{d}Y^2} + \mu\left(\frac{\mathrm{d}U}{\mathrm{d}Y}\right)^2 = 0. \tag{6}$$

By taking the derivative of Eqs. (1) and (2) with respect to $X$, one obtains

$$\frac{\partial^2 P}{\partial X^2} = 0, \quad \frac{\partial^2 P}{\partial X\partial Y} = 0. \tag{7}$$

The most general form of the function $P(X,Y)$ which fulfils Eq. (7) is as follows:

$$P(X,Y) = F(Y) + CX, \tag{8}$$

where $F(Y)$ is any function of $Y$ and $C$ is an arbitrary constant. By substituting Eq. (8) in Eqs. (1) and (2), one obtains

$$\mu\frac{\mathrm{d}^2U}{\mathrm{d}Y^2} + \rho_0 g\beta(T - T_0)\cos\varphi - C = 0, \tag{9}$$

$$\frac{\mathrm{d}F}{\mathrm{d}Y} - \rho_0 g\beta(T - T_0)\sin\varphi = 0. \tag{10}$$

The boundary conditions are:

$$U(-L) = U(L) = 0, \tag{11}$$

$$T(-L) = T_1, \quad T(L) = T_2. \tag{12}$$

## 3. Effect of buoyancy forces: analysis

In this section, starting from the solution for forced convection with viscous dissipation, the effect of buoyancy forces is analysed by means of a perturbation expansion. Let us define the dimensionless quantities

$$\begin{aligned}
&\lambda = -\frac{L^2}{\mu U_0}C, \quad \theta = \frac{T - T_0}{\Delta T}, \quad u = \frac{U}{U_0},\\
&y = \frac{Y}{L}, \quad Re = \frac{4LU_0\rho_0}{\mu},\\
&Gr = \frac{64\rho_0^2 g\beta L^3\Delta T}{\mu^2}, \quad Br = \frac{\Delta T}{T_2 - T_1},\\
&\eta = \frac{T_1 - T_0}{\Delta T}, \quad \varepsilon = \frac{Gr\cos\varphi}{Re},
\end{aligned} \tag{13}$$

where the mean velocity $U_0$ and the reference temperature difference $\Delta T$ are given by

$$U_0 = \frac{1}{2L}\int_{-L}^{L} U(Y)\,\mathrm{d}Y, \quad \Delta T = \frac{\mu U_0^2}{k}. \tag{14}$$

By introducing the dimensionless quantities in Eqs. (6) and (9), one obtains

$$\frac{\mathrm{d}^2u}{\mathrm{d}y^2} = -\frac{\varepsilon}{16}\theta - \lambda, \tag{15}$$

$$\frac{\mathrm{d}^2\theta}{\mathrm{d}y^2} = -\left(\frac{\mathrm{d}u}{\mathrm{d}y}\right)^2. \tag{16}$$

Eqs. (4) and (14) yield two constraints on $u(y)$ and $\theta(y)$, namely

$$\int_{-1}^{1} u(y)\,\mathrm{d}y = 2, \tag{17}$$

$$\int_{-1}^{1} \theta(y)\,\mathrm{d}y = 0. \tag{18}$$

Moreover, Eqs. (11)–(13) yield the dimensionless boundary conditions

$$u(-1) = u(1) = 0, \tag{19}$$

$$\theta(-1) = \eta, \quad \theta(1) = \frac{1}{Br} + \eta. \tag{20}$$

For fixed values of $Br$ and $\varepsilon$, Eqs. (15) and (16), with the boundary conditions Eqs. (19) and (20) and the constraints Eqs. (17) and (18), determine $\lambda$ and $\eta$ and yield $u$ and $\theta$ as functions of $y$. Thus, if $Br$ and $\varepsilon$ are fixed, then $u(y)$, $\theta(y)$, $\lambda$ and $\eta$ are uniquely determined. The definitions of the friction factors $f_1$ and $f_2$ at the channel walls, as well as the relation between $f_1$, $f_2$ and $\lambda$, can be found in [10].

One can also define a Nusselt number at each channel wall, as follows:

$$\begin{aligned} Nu_1 &= -\frac{4L\mathrm{d}T/\mathrm{d}Y|_{Y=-L}}{T(-L) - T_0} = -\frac{4}{\eta}\left.\frac{\mathrm{d}\theta}{\mathrm{d}y}\right|_{y=-1}, \\ Nu_2 &= \frac{4L\mathrm{d}T/\mathrm{d}Y|_{Y=L}}{T(L) - T_0} = \frac{4Br}{1 + Br\eta}\left.\frac{\mathrm{d}\theta}{\mathrm{d}y}\right|_{y=1}. \end{aligned} \tag{21}$$

The Nusselt numbers defined by Eq. (21) are based on the choice of $T_0$ as the reference temperature to express the heat transfer between each wall and the fluid. This choice has been adopted in other studies of mixed convection in ducts [10,11,17].

The dependence of $P$ on $Y$ can be described by means of the function

$$\Omega(y) = \int_{-1}^{y} \theta(y')\,\mathrm{d}y'. \tag{22}$$

In fact, by employing Eqs. (4), (8), (10) and (13), one obtains

$$\Omega(y) = \frac{16L}{\varepsilon\mu U_0 \tan\varphi}[P(X,Y) - P(X,-L)]. \tag{23}$$

Indeed, the difference $[P(X,Y) - P(X,-L)]$ is independent of $X$, as shown by Eq. (8). Moreover, Eqs. (18) and (22) show that $\Omega(1) = 0$ and therefore $[P(X,L) = P(X,-L)]$, on account of Eq. (23). For $\varepsilon \to 0$, i.e. in the limit of forced convection, Eqs. (22) and (23) allow one to conclude that $P$ is independent of $Y$.

The solution of Eqs. (15) and (16) with the boundary conditions Eqs. (19) and (20) and the constraints Eqs. (17) and (18) is obtained, as in [10], by means of a perturbation method in which $u(y)$, $\theta(y)$, $\lambda$ and $\eta$ are expressed as power series with respect to the parameter $\varepsilon$.

For the lowest perturbation order $n = 0$ (forced convection with viscous dissipation), one obtains

$$\begin{aligned} u_0(y) &= \frac{3}{2}(1 - y^2), \quad \lambda_0 = 3, \\ \theta_0(y) &= -\frac{3}{4}y^4 + \frac{1}{2Br}y + \frac{3}{20}, \\ \eta_0 &= -\left(\frac{3}{5} + \frac{1}{2Br}\right). \end{aligned} \tag{24}$$

Eq. (24) yields

$$\begin{aligned} &f_1 Re = 24 = f_2 Re, \quad Nu_1 = \frac{20(1 + 6Br)}{5 + 6Br}, \\ &Nu_2 = \frac{20(1 - 6Br)}{5 - 6Br}, \\ &\Omega(y) = -\frac{3}{20}y^5 - \frac{1}{4Br}(1 - y^2) + \frac{3}{20}y. \end{aligned} \tag{25}$$

Clearly, Eq. (25) holds for $\varepsilon \to 0$, i.e. in the limit of forced convection. As it has been pointed out before, the function $\Omega(y)$ given by Eq. (25) is not related to the difference $[P(X,Y) - P(X,-L)]$, which is zero in forced convection regime.

For $n > 0$ one obtains:

$$\begin{aligned} u_n(y) = &-\frac{1}{16}\int_{-1}^{y}(y - y')\theta_{n-1}(y')\,\mathrm{d}y' + \frac{y+1}{32}\int_{-1}^{1}(1 - y') \\ &\times \theta_{n-1}(y')\,\mathrm{d}y' + \frac{\lambda_n}{2}(1 - y^2), \end{aligned} \tag{26}$$

$$\begin{aligned} \theta_n(y) = \eta_n + \frac{y+1}{2}\int_{-1}^{1}(1 - y')\left(\sum_{j=0}^{n}\frac{\mathrm{d}u_j(y')}{\mathrm{d}y'}\frac{\mathrm{d}u_{n-j}(y')}{\mathrm{d}y'}\right)\mathrm{d}y' \\ - \int_{-1}^{y}(y - y')\left(\sum_{j=0}^{n}\frac{\mathrm{d}u_j(y')}{\mathrm{d}y'}\frac{\mathrm{d}u_{n-j}(y')}{\mathrm{d}y'}\right)\mathrm{d}y', \end{aligned} \tag{27}$$

$$\lambda_n = -\frac{3}{64}\int_{-1}^{1}(1 - y'^2)\theta_{n-1}(y')\,\mathrm{d}y', \tag{28}$$

$$\eta_n = -\frac{1}{4}\int_{-1}^{1}(1 - y'^2)\left(\sum_{j=0}^{n}\frac{\mathrm{d}u_j(y')}{\mathrm{d}y'}\frac{\mathrm{d}u_{n-j}(y')}{\mathrm{d}y'}\right)\mathrm{d}y'. \tag{29}$$

The symbolic evaluation of $u_n(y)$, $\theta_n(y)$, $\lambda_n$ and $\eta_n$ has been performed by means of a proper iterative algorithm based on Eqs. (26)–(29). By employing a personal computer, the evaluation has been performed up to the 35th perturbation order, for several values of the Brinkman number. The perturbation series have a finite radius of convergence, which depends on $Br$. In other words, for every value of $Br$ there exists a positive real number $\varepsilon_{\max}$ such that the perturbation series converge if and only if $|\varepsilon| < \varepsilon_{\max}$. Clearly, the convergence becomes slower when $|\varepsilon|$ approaches $\varepsilon_{\max}$. Nevertheless, perturbation series truncated to the 35th term ensure an excellent precision of the numerical results even for values of $|\varepsilon|$ rather close to $\varepsilon_{\max}$. The radius of convergence $\varepsilon_{\max}$ has been estimated by means of the method described in [11]. The following results have been obtained: $\varepsilon_{\max} \approx 7.4$ for $Br = 0.001$, $\varepsilon_{\max} \approx 24$ for $Br = 0.01$, $\varepsilon_{\max} \approx 77$ for $Br = 0.1$; $\varepsilon_{\max} \approx 200$ for $Br = 1$, $\varepsilon_{\max} \approx 240$ for $Br \geqslant 10$.

## 4. Effect of buoyancy forces: results

By employing the method described in Section 3, the friction factors, the dimensionless pressure drop, the Nusselt numbers, the dimensionless-velocity profile and the dimensionless-temperature profile have been evaluated, for some fixed values of $Br$, as functions of $\varepsilon$. The Grashof number $Gr$ defined in Section 3 is always positive. Therefore, negative values of $\varepsilon$ correspond to downward flow, while positive values correspond to upward flow. Moreover, as is shown by Eq. (13), for a fixed value of $Br$ an increase of $\varepsilon$ implies an increase of buoyancy effects. Finally, it is sufficient to report results for positive values of the Brinkman number, i.e. for $T_2 > T_1$. In fact, an analysis of Eqs. (13)–(21) shows that the change $Br \to -Br$, $\varepsilon \to \varepsilon$ implies: $u(y) \to u(-y)$, $\theta(y) \to \theta(-y)$, $\Omega(y) \to -\Omega(-y)$, $\lambda \to \lambda$, $f_1Re \to f_2Re$, $Nu_1 \to Nu_2$. Evaluations have been performed for several positive values of the Brinkman number. Some results for $Br = 0.1$ are reported in Fig. 2, where plots of the friction factors $f_1Re$ and $f_2Re$, of the mean value $(f_1Re + f_2Re)/2 = 8\lambda$, of the Nusselt numbers $Nu_1$ and $Nu_2$ are presented, in the range $-70 \leqslant \varepsilon \leqslant 70$. The figure shows that the dependence on $\varepsilon$ of the friction factors and of $\lambda$ is rather sharp. In particular, $f_1Re$ is a decreasing function of $\varepsilon$ and becomes negative for $\varepsilon \geqslant 25.6$; on the contrary, $f_2Re$ is an increasing function of $\varepsilon$ and is negative for $\varepsilon \leqslant -34.1$. The negative values of the friction factors are due to flow-reversal phenomena. The dimensionless pressure drop $\lambda$ is a decreasing function of $\varepsilon$, for every non-vanishing value of $Br$. For $Br = 0.1$, as is shown in Fig. 2, $\lambda$ decreases from 4.803 to 0.075 in the range $-70 \leqslant \varepsilon \leqslant 70$. In Fig. 2, plots of $Nu_1$ and $Nu_2$ versus $\varepsilon$ for $Br = 0.1$, in the interval $-70 \leqslant \varepsilon \leqslant 70$, are reported too. The dependence of $Nu_2$ on $\varepsilon$ is very strong. Indeed, $Nu_2$ is negative for $\varepsilon \geqslant 16.60$. As it will be shown in the following section, in the absence of viscous dissipation $\lambda$, $Nu_1$ and $Nu_2$ are not affected by buoyancy forces. Values of $\lambda$, $f_1Re$, $f_2Re$, $Nu_1$ and $Nu_2$ versus $\varepsilon$, for $Br = 0.01$ and for $Br = 0.1$, are reported in Table 1 with an accuracy of four digits.

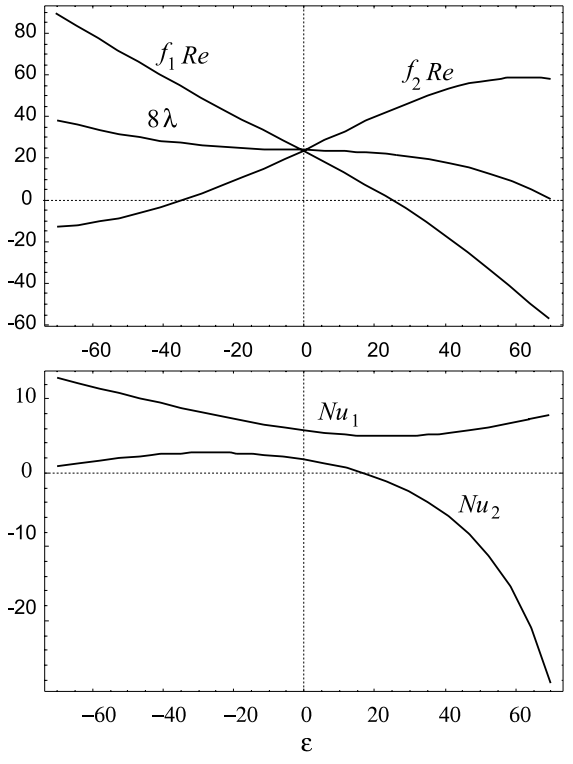


Fig. 2. Plots of $f_1Re$, $f_2Re$, $8\lambda$, $Nu_1$ and $Nu_2$ versus $\varepsilon$, for $Br = 0.1$, in the range $-70 \leqslant \varepsilon \leqslant 70$.

## 5. Effect of viscous dissipation: analysis

In this section, starting from the solution for mixed convection without viscous dissipation, the effect of viscous dissipation is analysed by means of a power-series expansion in which the perturbation parameter is the Brinkman number. Let us define the following dimensionless quantities, in addition to those defined in Eq. (13):

$$\theta_T = \frac{T - T_0}{T_2 - T_1}, \quad Gr_T = \frac{64\rho_0^2 g\beta L^3 (T_2 - T_1)}{\mu^2}, \quad \eta_T = \frac{T_1 - T_0}{T_2 - T_1}, \quad \varepsilon_T = \frac{Gr_T \cos\varphi}{Re}. \tag{30}$$

Clearly $\theta_T = Br\theta$, $Gr_T = Gr/Br$, $\eta_T = Br\eta$ and $\varepsilon_T = \varepsilon/Br$. From Eqs. (6), (9), (13) and (30) one obtains

$$\frac{d^2u}{dy^2} = -\frac{\varepsilon_T}{16}\theta_T - \lambda, \tag{31}$$

$$\frac{d^2\theta_T}{dy^2} = -Br\left(\frac{du}{dy}\right)^2. \tag{32}$$

The constraint on $u$ is still given by Eq. (17) and that on $\theta_T$ is

$$\int_{-1}^{1} \theta_T(y)\,dy = 0. \tag{33}$$

The dimensionless boundary condition for $u$ is still given by Eq. (19) and that on $\theta_T$ is

$$\theta_T(-1) = \eta_T, \quad \theta_T(1) = \eta_T + 1. \tag{34}$$

The Nusselt numbers are still defined by Eq. (21) and are expressed as

$$Nu_1 = -\frac{4}{\eta_T}\left.\frac{d\theta_T}{dy}\right|_{y=-1}, \quad Nu_2 = \frac{4}{1+\eta_T}\left.\frac{d\theta_T}{dy}\right|_{y=1}. \tag{35}$$

Table 1
Values of $\lambda$, $f_1Re$, $f_2Re$, $Nu_1$ and $Nu_2$ versus $\varepsilon$: in the range $-18 \leqslant \varepsilon \leqslant 18$ for $Br = 0.01$; in the range $-60 \leqslant \varepsilon \leqslant 60$ for $Br = 0.1$

| $Br = 1/100$ | | | | | | $Br = 1/10$ | | | | | |
|---|---|---|---|---|---|---|---|---|---|---|---|
| $\varepsilon$ | $\lambda$ | $f_1Re$ | $f_2Re$ | $Nu_1$ | $Nu_2$ | $\varepsilon$ | $\lambda$ | $f_1Re$ | $f_2Re$ | $Nu_1$ | $Nu_2$ |
| −18 | 6.358 | 194.0 | −92.26 | 8.719 | 0.8859 | −60 | 4.297 | 79.75 | −11.00 | 11.67 | 1.599 |
| −15 | 5.051 | 161.6 | −80.77 | 7.625 | 1.920 | −50 | 3.872 | 69.68 | −7.729 | 10.49 | 2.143 |
| −12 | 4.106 | 130.9 | −65.18 | 6.619 | 2.747 | −40 | 3.541 | 59.89 | −3.239 | 9.340 | 2.529 |
| −9 | 3.497 | 102.0 | −46.08 | 5.741 | 3.354 | −30 | 3.304 | 50.49 | 2.377 | 8.258 | 2.722 |
| −6 | 3.167 | 74.96 | −24.28 | 5.025 | 3.735 | −20 | 3.151 | 41.47 | 8.944 | 7.271 | 2.692 |
| −3 | 3.033 | 49.18 | −0.6446 | 4.501 | 3.888 | −10 | 3.059 | 32.70 | 16.24 | 6.411 | 2.405 |
| 0 | 3.000 | 24.00 | 24.00 | 4.190 | 3.806 | 0 | 3.000 | 24.00 | 24.00 | 5.714 | 1.818 |
| 3 | 2.966 | −1.359 | 48.82 | 4.110 | 3.478 | 10 | 2.939 | 15.08 | 31.94 | 5.220 | 0.8698 |
| 6 | 2.824 | −27.74 | 72.93 | 4.272 | 2.884 | 20 | 2.832 | 5.608 | 39.71 | 4.972 | −0.5393 |
| 9 | 2.463 | −55.94 | 95.35 | 4.677 | 1.993 | 30 | 2.631 | −4.752 | 46.85 | 5.010 | −2.570 |
| 12 | 1.773 | −86.58 | 114.9 | 5.313 | 0.7637 | 40 | 2.283 | −16.28 | 52.81 | 5.357 | −5.498 |
| 15 | 0.6681 | −119.9 | 130.6 | 6.150 | −0.8572 | 50 | 1.744 | −29.05 | 56.96 | 5.999 | −9.830 |
| 18 | −0.8944 | −155.5 | 141.2 | 7.140 | −2.935 | 60 | 0.9979 | −42.83 | 58.79 | 6.880 | −16.65 |

The dependence of $P$ on $Y$ can be described by means of the function

$$\Omega_T(y) = \int_{-1}^{y} \theta_T(y')\,\mathrm{d}y' \tag{36}$$

and of the relation

$$\Omega_T(y) = \frac{16L}{\varepsilon_T \mu U_0 \tan\varphi}[P(X,Y) - P(X,-L)]. \tag{37}$$

A solution of Eqs. (31) and (32), together with the boundary conditions Eqs. (19) and (34) and the constraints Eqs. (17) and (33), can be obtained by means of a perturbation method in which $u(y)$, $\theta_T(y)$, $\lambda$ and $\eta_T$ are expressed as power series with respect to $Br$, namely

$$u(y) = u_{T_0}(y) + u_{T_1}(y)Br + u_{T_2}(y)Br^2 + \cdots = \sum_{n=0}^{\infty} u_{T_n}(y)Br^n, \tag{38}$$

$$\theta_T(y) = \theta_{T_0}(y) + \theta_{T_1}(y)Br + \theta_{T_2}(y)Br^2 + \cdots = \sum_{n=0}^{\infty} \theta_{T_n}(y)Br^n, \tag{39}$$

$$\lambda = \lambda_{T_0} + \lambda_{T_1}Br + \lambda_{T_2}Br^2 + \cdots = \sum_{n=0}^{\infty} \lambda_{T_n}Br^n, \tag{40}$$

$$\eta_T = \eta_{T_0} + \eta_{T_1}Br + \eta_{T_2}Br^2 + \cdots = \sum_{n=0}^{\infty} \eta_{T_n}Br^n. \tag{41}$$

As in Section 3, one evaluates by an iterative procedure [10] the functions $u_{T_n}(y)$, $\theta_{T_n}(y)$ and the parameters $\lambda_{T_n}$ and $\eta_{T_n}$.

For $n = 0$ (mixed convection without viscous dissipation), one obtains:

$$u_{T_0}(y) = \frac{\varepsilon_T}{192}(y - y^3) + \frac{3}{2}(1 - y^2), \quad \lambda_{T_0} = 3, \quad \theta_{T_0}(y) = \frac{1}{2}y, \quad \eta_{T_0} = -\frac{1}{2}. \tag{42}$$

Eq. (42) yields

$$f_1Re = 24 - \frac{\varepsilon_T}{12}, \quad f_2Re = 24 + \frac{\varepsilon_T}{12}, \quad Nu_1 = Nu_2 = 4, \quad \Omega_T(y) = \frac{y^2 - 1}{4}. \tag{43}$$

Clearly, Eq. (43) holds for $Br \to 0$, i.e. in the limit of mixed convection without viscous dissipation.

For $n > 0$ one obtains:

$$\eta_{T_n} = -\frac{1}{4}\int_{-1}^{1}(1 - y'^2)\left(\sum_{j=0}^{n-1}\frac{\mathrm{d}u_{T_j}(y')}{\mathrm{d}y'}\frac{\mathrm{d}u_{T_{n-1-j}}(y')}{\mathrm{d}y'}\right)\mathrm{d}y', \tag{44}$$

$$\theta_{T_n}(y) = \eta_{T_n} + \frac{y+1}{2}\int_{-1}^{1}(1 - y')\times\left(\sum_{j=0}^{n-1}\frac{\mathrm{d}u_{T_j}(y')}{\mathrm{d}y'}\frac{\mathrm{d}u_{T_{n-1-j}}(y')}{\mathrm{d}y'}\right)\mathrm{d}y' - \int_{-1}^{y}(y - y')\left(\sum_{j=0}^{n-1}\frac{\mathrm{d}u_{T_j}(y')}{\mathrm{d}y'}\frac{\mathrm{d}u_{T_{n-1-j}}(y')}{\mathrm{d}y'}\right)\mathrm{d}y', \tag{45}$$

$$\lambda_{T_n} = -\frac{3}{64}\varepsilon_T\int_{-1}^{1}(1 - y'^2)\theta_{T_n}(y')\,\mathrm{d}y', \tag{46}$$

$$u_{T_n}(y) = -\frac{\varepsilon_T}{16}\int_{-1}^{y}(y - y')\theta_{T_n}(y')\,\mathrm{d}y' + \frac{\varepsilon_T}{32}(y+1)\times\int_{-1}^{1}(1 - y')\theta_{T_n}(y')\,\mathrm{d}y' + \frac{\lambda_{T_n}}{2}(1 - y^2). \tag{47}$$

The symbolic evaluation of $\eta_{T_n}$, $\theta_{T_n}(y)$, $\lambda_{T_n}$ and $u_{T_n}(y)$ has been performed, by means of a personal computer, up to the 28th perturbation order, for several values of $\varepsilon_T$. The perturbation series defined by Eqs. (38)–(41) have a finite radius of convergence $Br_{\max}$, which depends on $\varepsilon_T$ and has been estimated by means of the method described in [11]. The following results have been obtained: $Br_{\max} \approx 4.8$ for $\varepsilon_T = \pm 50$, $Br_{\max} \approx 2.4$ for $\varepsilon_T = \pm 100$, $Br_{\max} \approx 0.23$ for $\varepsilon_T = \pm 500$, $Br_{\max} \approx 0.062$ for $\varepsilon_T = \pm 1000$.

## 6. Effect of viscous dissipation: results

By employing the method described in Section 5, the friction factors, the dimensionless pressure drop, the Nusselt numbers, the dimensionless velocity profile and the dimensionless temperature profile have been evaluated, for some fixed values of $\varepsilon_T$, as functions of $Br$. Only positive values of $\varepsilon_T$ have been considered. The results for negative values of $\varepsilon_T$ can be obtained as follows. If one performs the change $\varepsilon_T \to -\varepsilon_T$ and $Br \to -Br$, the parameter $\varepsilon$ defined in Section 3 remains unchanged. Therefore, as we have shown in Section 4, $u(y) \to u(-y)$, $\theta(y) \to \theta(-y)$, $\Omega(y) \to -\Omega(-y)$, $\lambda \to \lambda$, $f_1 Re \to f_2 Re$, $Nu_1 \to Nu_2$. Note that, if $\varepsilon_T$ is positive, then $Br > 0$ corresponds to upward flow while $Br < 0$ corresponds to downward flow.

Some results for $\varepsilon_T = 100$ are presented in Figs. 3 and 4. Plots of $u$ and of $\theta_T$ versus $y$ are reported in Fig. 3 for $Br = 0$, $Br = 2$ and $Br = -2$. As pointed out by this figure, the effect of viscous dissipation on the velocity profile, in the range $-2 \leqslant Br \leqslant 2$, is rather sharp and is more significant for upward flow; a flow reversal due to the combined action of buoyancy and viscous dissipation occurs in a very thin layer close to the cold wall, for $Br = 2$. The effect of viscous dissipation on the dimensionless temperature profile, in the range $-2 \leqslant Br \leqslant 2$, is very sharp, especially for upward flow. Finally, Fig. 4 shows that viscous dissipation has a considerable influence on the distribution of the dimensionless pressure $\Omega_T(y)$.

Results for $\varepsilon_T = 1000$, in the range $-0.05 \leqslant Br \leqslant 0.05$, are presented in Figs. 5 and 6. Plots of $f_1 Re$, $f_2 Re$, $8\lambda$, $Nu_1$ and $Nu_2$ versus $Br$ are reported in Fig. 5. They show that the dependence of the friction factors on $Br$ is sharp and that $\lambda$ becomes negative for $Br \geqslant 0.041$. The dependence of $Nu_1$ and $Nu_2$ on $Br$ is very sharp too, and $Nu_2$ is negative for $Br \geqslant 0.016$. Fig. 6 shows that viscous dissipation enhances the flow reversal close to the wall at $y = -1$ for $Br > 0$ (upward flow, $T_1 < T_2$) and inhibits it for $Br < 0$ (downward flow, $T_1 > T_2$). The same figure illustrates also the effect of the Brinkman number on the dimensionless temperature profile and explains why $Nu_2$ is negative for $Br = 0.05$: at $y = 1$, the heat flux goes out of the channel and $T(L) > T_0$.

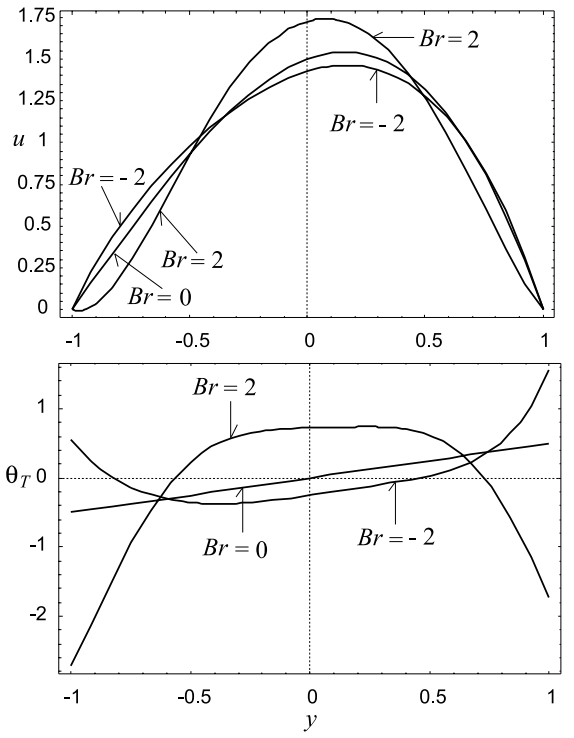


Fig. 3. Plots of $u$ and $\theta_T$ versus $y$, for $\varepsilon_T = 100$ and $Br = 0$, $Br = -2$, $Br = 2$.

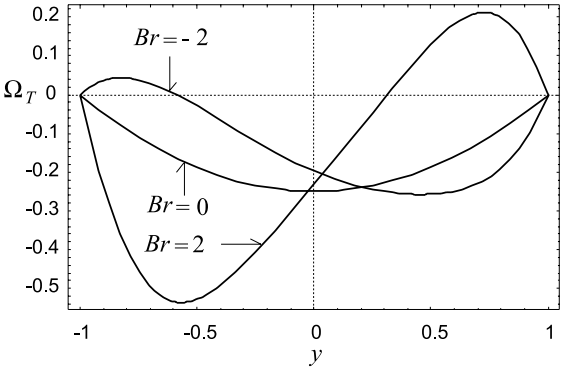


Fig. 4. Plots of $\Omega_T$ versus $y$, for $\varepsilon_T = 100$ and $Br = 0$, $Br = -2$, $Br = 2$.

Values of $\lambda$, $f_1 Re$, $f_2 Re$, $Nu_1$ and $Nu_2$ versus $Br$, for $\varepsilon_T = 100$ and for $\varepsilon_T = 1000$, are reported in Table 2 with an accuracy of four digits. These values have been checked by employing the perturbation method described in Section 3: the same results have been found.

The results described in this section, as well as those presented in Section 4, point out that buoyancy forces enhance the effect of viscous dissipation and vice versa.

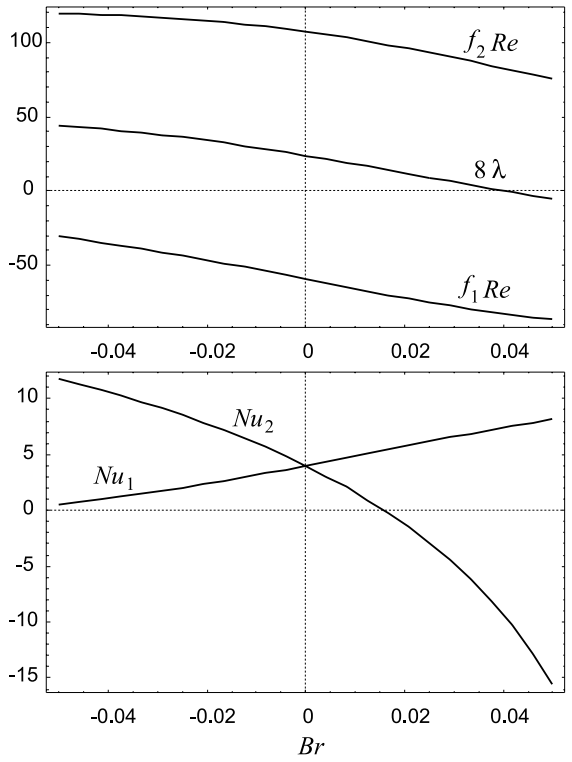


Fig. 5. Plots of $f_1Re$, $f_2Re$, $8\lambda$, $Nu_1$ and $Nu_2$ versus $Br$, for $\varepsilon_T = 1000$, in the range $-0.05 \leqslant Br \leqslant 0.05$.

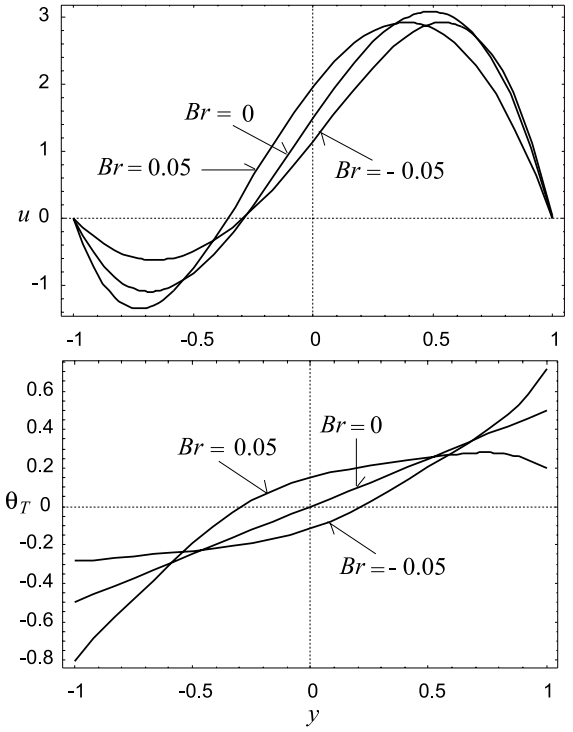


Fig. 6. Plots of $u$ and $\theta_T$ versus $y$, for $\varepsilon_T = 1000$ and $Br = 0$, $Br = -0.05$, $Br = 0.05$.

Table 2
Values of $\lambda$, $f_1Re$, $f_2Re$, $Nu_1$ and $Nu_2$ versus $Br$: in the range $-1.4 \leqslant Br \leqslant 1.4$ for $\varepsilon_T = 100$; in the range $-0.035 \leqslant Br \leqslant 0.035$ for $\varepsilon_T = 1000$

| $\varepsilon_T = 100$ | | | | | | $\varepsilon_T = 1000$ | | | | | |
|---|---|---|---|---|---|---|---|---|---|---|---|
| $Br$ | $\lambda$ | $f_1Re$ | $f_2Re$ | $Nu_1$ | $Nu_2$ | $Br$ | $\lambda$ | $f_1Re$ | $f_2Re$ | $Nu_1$ | $Nu_2$ |
| −1.4 | 3.665 | 22.32 | 36.32 | 41.64 | 18.89 | −0.035 | 4.986 | −37.91 | 117.7 | 1.413 | 9.947 |
| −1.2 | 3.586 | 21.52 | 35.86 | 53.40 | 17.84 | −0.03 | 4.762 | −40.64 | 116.8 | 1.728 | 9.262 |
| −1.0 | 3.503 | 20.67 | 35.38 | 98.30 | 16.64 | −0.025 | 4.519 | −43.51 | 115.8 | 2.063 | 8.532 |
| −0.8 | 3.415 | 19.78 | 34.87 | −199.0 | 15.21 | −0.02 | 4.255 | −46.50 | 114.6 | 2.416 | 7.752 |
| −0.6 | 3.322 | 18.84 | 34.31 | −26.90 | 13.48 | −0.015 | 3.970 | −49.60 | 113.1 | 2.787 | 6.916 |
| −0.4 | 3.222 | 17.85 | 33.71 | −7.139 | 11.29 | −0.01 | 3.666 | −52.79 | 111.4 | 3.177 | 6.017 |
| −0.2 | 3.115 | 16.79 | 33.06 | 0.2599 | 8.344 | −0.005 | 3.342 | −56.04 | 109.5 | 3.582 | 5.048 |
| 0 | 3.000 | 15.67 | 32.33 | 4.000 | 4.000 | 0 | 3.000 | −59.33 | 107.3 | 4.000 | 4.000 |
| 0.2 | 2.875 | 14.47 | 31.53 | 6.173 | −3.418 | 0.005 | 2.643 | −62.62 | 104.9 | 4.429 | 2.863 |
| 0.4 | 2.738 | 13.19 | 30.62 | 7.540 | −20.30 | 0.01 | 2.274 | −65.86 | 102.3 | 4.864 | 1.623 |
| 0.6 | 2.588 | 11.82 | 29.59 | 8.443 | −113.3 | 0.015 | 1.897 | −69.03 | 99.38 | 5.302 | 0.2664 |
| 0.8 | 2.421 | 10.34 | 28.40 | 9.063 | 113.4 | 0.02 | 1.516 | −72.07 | 96.32 | 5.740 | −1.229 |
| 1.0 | 2.235 | 8.743 | 27.02 | 9.506 | 51.32 | 0.025 | 1.134 | −74.96 | 93.11 | 6.172 | −2.889 |
| 1.2 | 2.024 | 6.998 | 25.38 | 9.837 | 36.61 | 0.03 | 0.7564 | −77.68 | 89.78 | 6.597 | −4.751 |
| 1.4 | 1.780 | 5.064 | 23.42 | 10.10 | 29.45 | 0.035 | 0.3852 | −80.20 | 86.36 | 7.011 | −6.865 |

## 7. Conclusions

Two different perturbation expansions have been employed to study the fully developed laminar mixed convection in an inclined channel with prescribed wall temperatures. The different methods have allowed a cross check of the results. Moreover, they have allowed an analysis of the effects of buoyancy forces for given values of the Brinkman number, as well as of the effects of viscous dissipation for given values of the Grashof

number. Evaluations have been performed by a symbolic algorithm which employs rational numbers, thus avoiding rounding off errors. The results obtained are very accurate, in the domain of validity of the assumptions which characterise the mathematical model. The results point out that viscous dissipation enhances the effects of buoyancy and vice versa. In particular, only in the presence of viscous dissipation the dimensionless pressure drop coefficient $\lambda$ and the Nusselt numbers have been shown to depend sharply on the Grashof number. In the presence of buoyancy forces, viscous dissipation affects and may produce flow-reversal phenomena. Finally, the combined effects of buoyancy and dissipation may yield negative values of the dimensionless pressure drop coefficient $\lambda$.

## References


[1] W. Aung, Mixed convection in internal flow, in: S. Kakaç, R.K. Shah, W. Aung (Eds.), Handbook of Single-Phase Convective Heat Transfer, Wiley, New York, 1987 (Chapter 15).

[2] W. Aung, G. Worku, Theory of fully developed, combined convection including flow reversal, ASME J. Heat Transfer 108 (1986) 485–488.

[3] C.-H. Cheng, H.S. Kou, W.H. Huang, Flow reversal and heat transfer of fully developed mixed convection in vertical channels, J. Thermophys. Heat Transfer 4 (1990) 375–383.

[4] T.T. Hamadah, R.A. Wirtz, Analysis of laminar fully developed mixed convection in a vertical channel with opposing buoyancy, ASME J. Heat Transfer 113 (1991) 507–510.

[5] A. Barletta, E. Zanchini, On the choice of the reference temperature for fully developed mixed convection in a vertical channel, Int. J. Heat Mass Transfer 42 (1999) 3169–3181.

[6] Y.-C. Chen, J.N. Chung, The linear stability of mixed convection in a vertical channel flow, J. Fluid Mech. 325 (1996) 29–51.

[7] Y.-C. Chen, J.N. Chung, Stability of mixed convection in a differentially heated vertical channel, ASME J. Heat Transfer 120 (1998) 127–132.

[8] A. Barletta, Laminar mixed convection with viscous dissipation in a vertical channel, Int. J. Heat Mass Transfer 41 (1998) 3501–3513.

[9] A. Barletta, Combined forced and free convection with viscous dissipation in a vertical circular duct, Int. J. Heat Mass Transfer 42 (1999) 2243–2253.

[10] A. Barletta, Analysis of combined forced and free flow in a vertical channel with viscous dissipation and isothermal–isoflux boundary conditions, ASME J. Heat Transfer 121 (1999) 349–356.

[11] A. Barletta, Heat transfer by fully developed flow and viscous heating in a vertical channel with prescribed wall heat fluxes, Int. J. Heat Mass Transfer 42 (1999) 3873–3885.

[12] E. Zanchini, Effect of viscous dissipation on mixed convection in a vertical channel with boundary conditions of the third kind, Int. J. Heat Mass Transfer 41 (1998) 3949–3959.

[13] A.S. Lavine, Analysis of fully developed opposing mixed convection between inclined parallel plates, Wärme- und Stoffübertragung 23 (1988) 249–257.

[14] A.S. Lavine, On the linear stability of mixed and free convection between inclined parallel plates with fixed heat flux boundary conditions, Int. J. Heat Mass Transfer 36 (1993) 1373–1387.

[15] A.S. Lavine, M.Y. Kim, C.N. Shores, Flow reversal in opposing mixed convection flow in inclined pipes, ASME J. Heat Transfer 111 (1989) 114–120.

[16] D. Choudury, S.V. Patankar, Combined forced and free laminar convection in the entrance region of an inclined isothermal tube, ASME J. Heat Transfer 110 (1988) 901–909.

[17] B.R. Morton, Laminar convection in uniformly heated vertical pipes, J. Fluid Mech. 8 (1960) 227–240.